# SOM-based Visualization Monitoring and Fault Diagnosis for Chemical Process

Bin Zhong, Jing Wang, Haiyan Wu, Jinglin Zhou and Qibing Jin

College of Information Science and Technology, Beijing University of Chemical Technology, Beijing 100029, China
E-mail: jwang@mail.buct.edu.cn

**Abstract:** Data-based fault diagnosis technology applied in chemical industry process has attracted great attention, in which the effective methods for visualizing the process variation are still challenging. The self-organizing map (SOM) is an unsupervised learning algorithm of neural network, which is presented to solve the visualization monitoring and fault diagnosis problem. The high-dimensional input space is mapped to the two-dimensional output space through training the large sample data sets of SOM method. Meanwhile, the fault data sets can be automatically clustering by SOM so that the faulty category information will be obtained. Distinguish between other methods, SOM can preserve the topological structure and the density distribution of original data, so the visualization of on-line process monitoring and fault diagnosis can be effectively realized. Then, the Iris data benchmark is used to test the clustering results of SOM algorithm. Finally, a case study of the Tennessee Eastman (TE) process is employed to illustrate the fault diagnosis and monitoring performance of the SOM-based visualization monitoring method.

**Key Words:** Self-organizing Map (SOM), On-line Process Monitor, Visualization, Information Cluster, Fault Diagnosis

## 1    INTRODUCTION

Nowadays, it is more complex for the structure of modern industrial process and mechanical equipment. It would be produced a chain reaction when once the fault occur. In addition, the bigger the scale of the process, the more difficult for the operator to find the cause of the problem and troubleshoot it in time. Therefore, it has important practical significance to research fault diagnosis and condition monitoring technology for chemical equipment and production process [1-2].

To work out the process monitoring and fault diagnosis problem, the process industry mainly adopts the following method for the moment. (1) Using single variable process control (SPC) or multivariate statistical process monitoring (MSPM) method for process monitoring. CUSUM (cumulative sum) [3] and EWMA (exponentially weighted moving-average) control charts [4] are commonly used methods of SPC. PCA (principal component analysis) [5-7], FDA (fisher discriminant analysis) [8-9] and PLS (partial least squares) [10-12] are the representative methods of the MSPM. A lot of process variables and the serious correlation between the variables lead to the disadvantages for the SPC, and make MSPM get a long-term development. (2) Qualitative expert system [13-14], quantitative multivariate statistical method [15-16] and clustering method [17-18] are adopted to solve the problem of fault diagnosis. The data driven technology of PCA, FDA, PLS and their extended methods, are both to use $T^2$ and $SPE$ statistics and their corresponding control limits to monitor the changes of process [19]. However, these methods are not to provide a kind of visual graphics to visualize the online process for process monitoring and fault diagnosis. It prompts the rapid application of SOM (self-organizing map) visualization method in the fault diagnosis field.

SOM is a machine learning method which belongs to the category of the data driven fault diagnosis method. SOM has been widely used in the chemical process fault diagnosis since it clusters the process data sets effectively [20]. What's more, SOM can deal with large quantities of high-dimensional data sets quickly and availably. The mapping result is easy to visualization. In this paper, the Iris data benchmark is firstly used to test the clustering results of SOM algorithm. Then, a case study of the Tennessee Eastman (TE) process is employed to illustrate the fault diagnosis and monitoring performance of the SOM-based visualization monitoring method. Grayscale of U matrix, hit histogram, distance matrix and label plan are used to show the effect of the SOM intuitively for clustering and fault diagnosis. At the same time, dynamic trajectory graph is used to monitor the dynamic change for industrial process.

## 2    The SOM-based Visualization Monitoring and Fault Diagnosis

### 2.1  The SOM network

The SOM algorithm of neural network is put forward by professor Kohonen [21]. It can be used the topological structure to achieve dimension reduction mapping from a n-dimensional input space to a two- dimensional output space. The network structure of SOM is shown in Figure 1, which consists of input layer and output layer. The input layer is corresponding to a high-dimensional input vectors, and the output layer is made up of a series of orderly nodes on the two-dimensional grid. Through the weight vectors, the input nodes are connected to the output nodes.

During the training step, we try to find and update the output layer unit which has the shortest distance between the input vector and the weight vector. It was named as best matching unit (BMU) [22]. The BMU is the best mapping for the input samples.
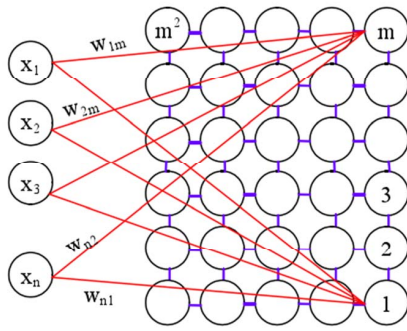
Fig 1. Network structure of SOM

The "Mexican hat wavelet" function is shown as Figure 2, which explains the response mechanism of SOM. When input a certain mode, the BMU is as the center of the circle, the neighboring neurons show excitability feedback, while the neurons of distant neighbors show inhibitory feedback. Thereby, the weight vector of the neuron is corrected towards the direction of the input pattern. Once the input mode changes, the winning neuron of the output plane also shifts to others.
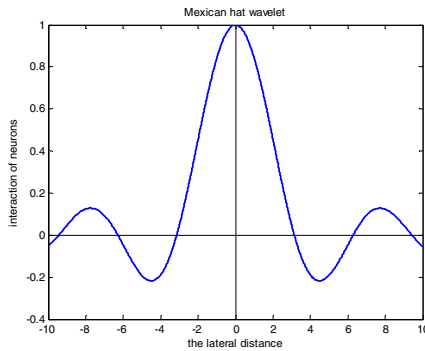


Fig 2. Mexican hat wavelet function

Through this kind of response mechanism, a large number of training samples are input to the network and the weight vectors are adjusted constantly in order to keep the output layer reflect the original space distribution of sample data.

## 2.2 The SOM visual tool for process monitoring and fault diagnosis

Each neuron of SOM network output layer has a two-dimensional coordinates. We can obtain a third-dimensional coordinate for the neuron, which is called as the neuron's "U" value by calculating the Euclidean distance of weight vector between one neuron and its adjacent neurons. So that we can draw a distance matrix chart in a three-dimensional space. The grayscale of U matrix represents the size of the "U" value.

SOM is a very good tool for high-dimensional data clustering using U matrix, histogram collision and other indexes to visual the data sets. In this paper, we use grayscale of U matrix, hit histogram, distance matrix and label plan to intuitively show the effect for clustering fault diagnosis. A dynamic trajectory graph is simultaneously used to monitor the dynamic change for industrial process.

## 2.3 The SOM trained for visualization monitoring and fault diagnosis

Based on the above response mechanism of SOM, the concrete implementation steps are as follows.

(1) Initialize the weight vector $\{w_{ij}\}$, the initial values $\eta(0)$ of learning rate $\eta(t)$ and $N_g(0)$ of neighborhood field $N_g(t)$, the total number of learning $T$. Where $i = 1, 2, ..., S$, $j = 1, 2, ..., R$, $S$ is the number of output neurons. $N_g(t)$ refers to an area where the BMU of $g$ as the center and includes a number of neighboring neurons.

(2) Collect normal and fault condition data sets $P_k = (p_1^k, p_2^k, ..., p_R^k)$ as input mode and establish the process fault samples library. Here $k = 1, 2, ..., Q$ and $Q$ is total number of learning samples, $R$ is the sample dimension.

(3) Mark the BMU label for each class fault samples in the library. Calculate the Euclid distance $d_i$ between the connection weight vector $W = (w_{i1}, w_{i2}, ..., w_{iR})$ and the input mode $P_k = (p_1^k, p_2^k, ..., p_R^k)$ as follows:

$$d_i = [\sum_{j=1}^{R} (P_j^k - w_{ij})^2]^{1/2}, i = 1, 2, ..., S \quad (1)$$

Find the minimum distance $d_g$ and determine the $g$-th neuron as the BMU.

$$d_g = \min[d_i], i = 1, 2, ..., S \quad (2)$$

(4) The fault samples are clustered according to the input mode. The connection weight vector $w_{ij}$ is adjusted. The revised formulas are as follows:

$$w_{ij}(t+1) = w_{ij}(t) + \eta(t)(p_j^k - w_{ij}(t)), j = g \quad (3)$$

$$w_{ij}(t+1) = w_{ij}(T) + \eta(t)/2 \times (p_j^k - w_{ij}(t)), j = N_g(t) \quad (4)$$

$$w_{ij}(t+1) = w_{ij}(t), j \notin N_g(t) \quad (5)$$

(5) Provide another input samples to the input layer of the network. Then return to step (3) until the $Q$ learning samples are all provided to the network.

(6) Update $\eta(t)$ and $N_g(t)$.

$$\eta(t) = \eta(0) \times (1 - t/T) \quad (6)$$

$$N_g(t) = N_g(0) \times (1 - t/T) \quad (7)$$

(7) Increase the learning steps. Set $t=t+1$, and return to step (2) until $t=T$.

We will obtain weight vector $\{w_{ij}\}$, learning rate $\eta(t)$ and neighborhood field $N_g(t)$, which have been adjusted well through the SOM training model.

(8) Input a testing mode $P1_k = (p1_1^k, p1_2^k, ..., p1_r^k)$ to the SOM neural network, $r$ is the testing sample dimension. Compare the clustering results of the test mode with the normal operation and the known faults in training sample library to demonstrate whether the test sample is in failure or what kind of fault it belongs to.

# 3 CASE STUDY

It usually uses some real data set to verify the clustering and visualization capabilities of SOM, such as Iris, Breast-cancer, Wine and Zoo. In this paper, Iris data set and TE simulation process are utilized to review the clustering ability of SOM. Then, SOM is used to cluster several fault types and plot a dynamic trajectory graph to observe the online dynamic trajectory for the process. It is further validated the good performance of SOM visualization method for chemical process monitoring and fault diagnosis.

## 3.1 The clustering results analysis for Iris data set

Iris is a set of 4 attributes data. It includes 150 data samples and it is divided into three categories, each category has 50 data samples. The first 40 samples are used for training, and the rest for testing. It is linear separable between the first class and the other two classes in Iris data set. However, it is linear inseparable between the second and the third class. Figure 3 give the clustering results based on SOM method for these three categories data.
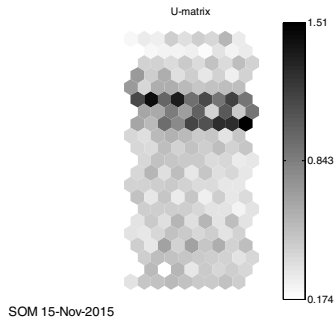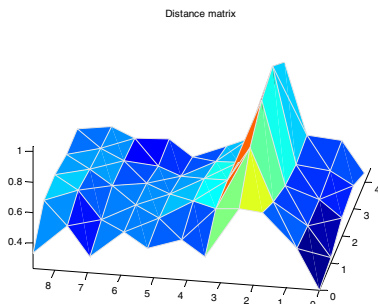


Fig 3. Grayscale of U matrix



Fig 4. Distance matrix

The gray distribution of U matrix, as shown in Figure 3, is used to represent the input vector clustering tendency. The gray area indicates a larger value of U matrix used to show a class boundary. Yet, the white area denotes a smaller value of U matrix used to display the clustering center. The boundary between the first class and the other two classes is particularly obvious shown in the grayscale of U matrix,. Figure 4 is corresponding to Figure 3, but displayed in a three-dimension space. The distance matrix value achieves to maximum in the vicinity of $x=3$, and it is the most obvious boundary in three kinds of Iris data set.
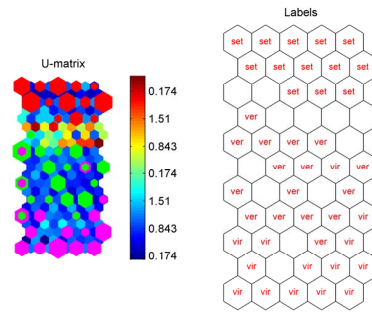


Fig 5. hit histogram(left) and label plan(right) for Iris

The SOM training results of hit histogram and label plan are shown as Figure 5(left) and (right). The size of the hexagon denotes the number of data samples projected to the output neurons. SOM can clearly separate the three categories of Iris data, which even can separate the two class samples of linear inseparable. The 98% correct rate is reached. Then, the trained network model of SOM is used to test. Figure 6 is the testing result of the last 10 samples for Iris. Three kinds of Iris data are clustered very well. It is demonstrated that SOM is a very good visualization tool for clustering different data set.
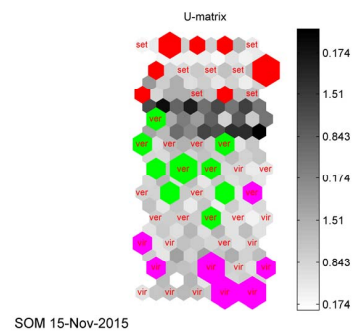


Fig 6. The SOM testing result for Iris

## 3.2 The monitoring and fault diagnosis results analysis for TE process

Tennessee Eastman (TE) process, a realistic simulation program of a chemical plant by Downs and Vogel [23], is a benchmark for control and monitoring studies.
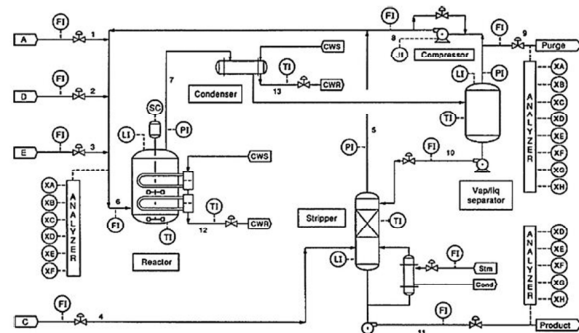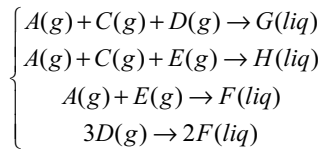


Fig 7. The TE process flow chart

The whole process consists of five main parts including separator, reactor, compressor, condenser and stripper as shown in Figure 7. It contains eight components, where gas

composition of A, C, D, E and inert component B are fed into the reactor. Liquid product G and H are products, and chemical reactions are as follows [23].

$$\begin{cases} A(g)+C(g)+D(g) \rightarrow G(liq) \\ A(g)+C(g)+E(g) \rightarrow H(liq) \\ \quad A(g)+E(g) \rightarrow F(liq) \\ \quad\quad 3D(g) \rightarrow 2F(liq) \end{cases}$$

TE process has 41 measurement variables, 12 manipulated variables and 21 preset faults. We use all measurement variables XMEAS(1)~XMEAS(41), 11 manipulated variables XMV(1)~XMV(11), only IDV(0) and five faults to verify the simulation result for SOM-based visualization method. IDV(0) is normal process and others are five faults of different abnormal operating conditions which seen in Table 1.

Table1. Fault types

| symbol | process variables | type |
| --- | --- | --- |
| IDV(0) | normal | ---- |
| IDV(1) | A/C feed ratio, B is constant | step |
| IDV(2) | B component, A/C feed ratio is constant | step |
| IDV(4) | reactor cooling water flow | step |
| IDV(6) | A feed loss | step |
| IDV(10) | C inlet temperature | random variable |

### 3.2.1 IDV(0), IDV(1) and IDV(2)

Firstly, we collect 80 samples of normal condition IDV(0), IDV(1) and IDV(2) from the TE simulation process, respectively. Secondly, the three training set are used to establish SOM network. The results are shown in Figure 8 and 9 to illustrate the performance of SOM-based method.
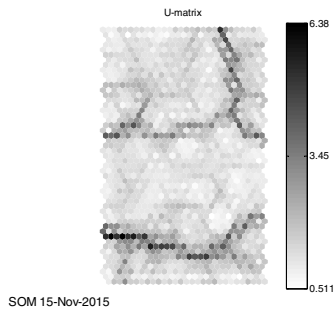


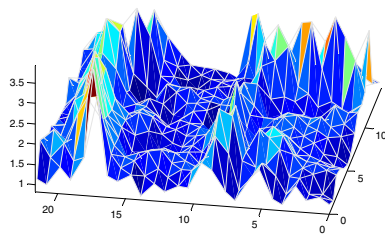Fig 8. Grayscale of U matrix for IDV(0), IDV(1) and IDV(2)



Fig 9. Distance matrix for IDV(0), IDV(1) and IDV(2)

From Figure 8 and Figure 9, one realizes that the darker part of Figure 8 is corresponding with the bigger height values

of distance matrix. The training results show that the input data are divided into three regions. To be more intuitive to show the clustering result of input data, we propose the labels plan to the mapping result of SOM network, although the SOM network is an unsupervised method. The results are shown in Figure 10.
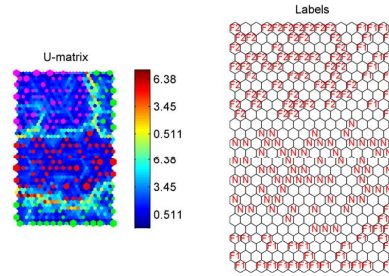


Fig 10. hit histogram(left) and label plan(right) for IDV(0), IDV(1) and IDV(2)

In the histogram, IDV(0), IDV(1) and IDV(2) is recognized by red, green and pink projection. The mapping results can clearly show that the output plane neurons are divided into three categories both in the hit histogram and the label plan. Moreover, the results have the 100% clustering accuracy, which means that this method can separate the normal operation condition and fault classes effectively.

The next is about the test results. The weights of network are fixed when the SOM network is trained well. Then we use the network to test the effectiveness of online process monitoring. We choose 10 test samples as the input of SOM network from each type of IDV(0), IDV(1) and IDV(2). Figure 11 shows the mapping result from input data to the output neurons and their dynamic motion curve.
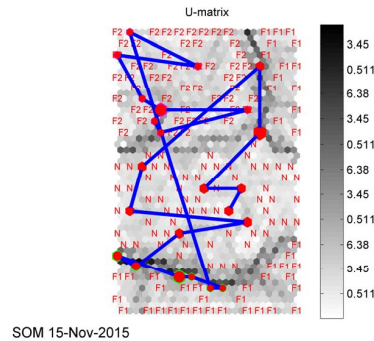


Fig 11. The dynamic trajectory graph for IDV(0), IDV(1) and IDV(2)

From the dynamic trajectory graph, we can observe the whole evolution route from normal to fault state. At first, all the observation samples are mapping in the "N" area where the normal condition is. Then the new BMU are mapped and the track is extended with the passage of time. The blue trajectory shifts from the normal region "N" to region "F1" and from "F1" to "F2". Therefore, we can get a real-time monitoring scene for industrial process by following this graph, and the occurrence of abnormal condition is detected on the monitor graph. Dynamic trajectory graph is mainly

used to verify the capacity of the SOM based method for clustering different process fault types and fault diagnosis.

### 3.2.2 IDV(0), IDV(1), IDV(2) and IDV(6)

In this section, the diagnosis results of SOM are checked for multiple fault types. From the TE simulation platform, we collect 80 samples of IDV(0), IDV(1)，IDV(2)and IDV(6) respectively, and the training samples are used to establish SOM network.
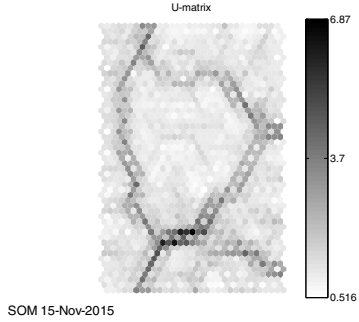


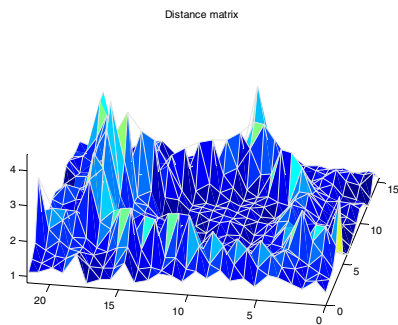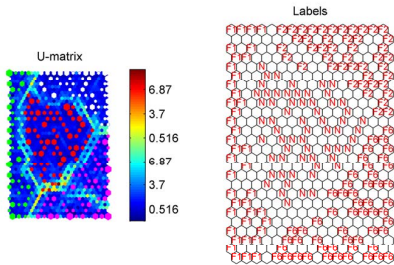Fig 12. Grayscale of U matrix for IDV(0), IDV(1), IDV(2) and IDV(6)



Fig 13. Distance matrix for IDV(0), IDV(1) , IDV(2) and IDV(6)

Figure 12 and Figure 13 show that dark color divided the input data sets into five types. Then, we draw the hit histogram and the label plan as shown in Figure 14.

Fig 14. Hit histogram(left) and label plan(right) for IDV(0), IDV(1), IDV(2) and IDV(6)

The input data sets are divided into 4 types shown in the hit histogram and label plan. What's more, from the clustering results, the SOM training model show 100% clustering accuracy that means this method can separate the normal operation condition and fault classes effectively. However, it is noting that SOM method can make mistake if we focus on a type visual graph only such as grayscale graph. Because the training data sets are four types but the grayscale shows five types. Thus, different visual graphs should be combining with each other to obtain the correct classification of process data sets availably.

The dynamic trajectory graph of each 10 test samples is shown in Figure 15. We note that a "F6" sample enters the "N" area, and five samples of "F1" are at the border between "F1" and "N" areas. But the input data sets of industry process are clearly divided into four classes from the view of the whole mapping result, and the process dynamic trajectory is from "N" to "F1", then "F1" to "F2", finally "F2" to "F6".
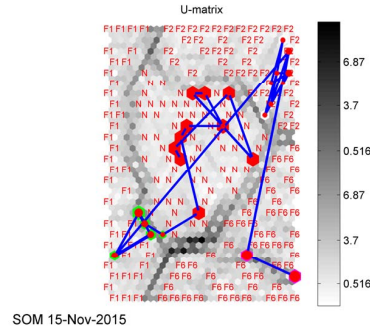


Fig 15. The dynamic trajectory graph for IDV(0), IDV(1), IDV(2) and IDV(6)

### 3.2.3 IDV(0), IDV(4) and IDV(10)

In this section, a different training set are tested for generalization. First, we collect 80 training samples of IDV(0), IDV(4) and IDV(10) from the TE simulation platform to establish SOM network, respectively. The mapping results of hit histogram and the intuitive label plan are shown in Figure 16.
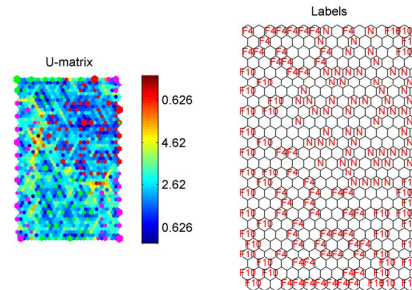


Fig 16. Hit histogram(left) and label plan(right) for IDV(0), IDV(4) and IDV(10)

From Figure 16, SOM network cannot distinguish fault data with the normal state. Why can appear such result？ The fault types of IDV(1), IDV(2) and IDV(6) are easy to diagnose relatively because more than half the number of the process variables are deviated from their normal operation threshold obviously once the fault happens. However, they will only cause subtle changes for process variables if IDV(4) and IDV(10) happen, and the SOM based method is invalid. Therefore, it is difficult to detect these different types of faults. This is a disadvantage for SOM and further improvement and research should be focused on it.

## 4 CONCLUSIONS

The SOM-based visualization monitoring and fault diagnosis for chemical process is presented in this paper. The detailed training steps are described or concluded. The effectiveness of SOM is proved by simulation results of Iris and TE process for process monitoring and fault diagnosis. Several visual graphs of SOM are used for clustering multiple fault types: the grayscale of U matrix, distance matrix, hit histogram, label plan and the dynamic trajectory. But the improvement of SOM based method is necessary for some faults which can cause subtle changes of process variables. SOM has great potential advantage as a powerful visualization tool, which is worth for further research in process monitoring and fault diagnosis.

## REFERENCES

[1] Tapan K. Saha, Review of modern diagnostic techniques for assessing insulation condition in aged transformers, IEEE Trans. on Dielectrics and Electrical Insulation, Vol.10, No.5, 903-917, 2003.

[2] Xueqin Liu, Lei Xie, Uwe Kruger, Tim Littler, Shuqing Wang, Statistical-Based Monitoring of Multivariate Non-Gaussian Systems, AIChE Journal, Vol.54, No.9, 2379-2391, 2008.

[3] Olha Bodnar , Wolfgang Schmid, CUSUM charts for monitoring the mean of a multivariate Gaussian process, Journal of Statistical Planning and Inference, Vol.141, No.6, 2055-2070, 2011.

[4] Marion R. Reynolds, Jesse C. Arnold, EWMA control charts with variable sample sizes and variable sampling intervals, IIE Transactions, Vol.33, No.6, 511-530, 2001.

[5] J. Edward Jackson, A User's Guide to Principal Components, New York: Wiley, 2005.

[6] Tiago J. Rato, Marco S. Reis, Advantage of Using Decorrelated Residuals in Dynamic Principal Component Analysis for Monitoring Large-Scale Systems, Ind. Eng. Chem. Res., Vol.52, No.38, 13685-13698, 2013.

[7] Wenshuang Ge, Jing Wang, Jinglin Zhou, Haiyan Wu, Qibing Jin, Incipient Fault Detection Based on Fault Extraction and Residual Evaluation, Ind. Eng. Chem. Res., Vol.54, No.14, 3664-3677, 2015.

[8] Liying Jiang, Shuqing Wang, Monitoring and fault diagnosis of batch processes using multi-model fisher discriminant analysis, Intelligent Control and Automation, Vol.2, 1780-1784, 2004.

[9] Xi Zhang, Sile Ma, Weiwu Yan, Xu Zhao, Huihe Shao, A novel systematic method of quality monitoring and prediction based on FDA and kernel regression, Chinese J of Chemical Engineering, Vol.17, No.3, 427-436, 2009.

[10] S. Joe Qin, Yingying Zheng, Quality-Relevant and Process-Relevant Fault Monitoring with Concurrent Projection to Latent Structures, AIChE Journal, Vol.59, No.2, 496-504, 2013.

[11] Samia Samar Ouertani, Gérard Mazerolles, Julien Boccard, Serge Rudaz, Mohamed Hanafi, Multi-way PLS for discrimination: Compact form equivalent to the tri-linear PLS2 procedure and its monotony convergence, Chemom Intell. Lab Syst., Vol.133, 25-32, 2014.

[12] Bo Lu, Ivan Castillo, Leo Chiang, Thomas F. Edgar, Industrial PLS model variable selection using moving window variable importance in projection, Chemom. Intell. Lab. Syst., Vol.135, 90-109, 2014.

[13] C. Angeli, Online expert system for fault diagnosis in hydraulic systems, Expert systems, Vol.16, No.2, 115-120, 1999.

[14] Sandhya Samarasinghe, Neural networks for applied sciences and engineering-From fundamentals to complex pattern recognition, China Machine Press, 2010.

[15] S. Joe Qin, Statistical process monitoring: Basics and beyond, J. Chemometr, Vol.17, 480-502, 2003.

[16] Tao Chen, Jie Zhang, On-line multivariate statistical monitoring of batch processes using Gaussian mixture model, Comput. Chem. Eng., Vol.34, No.4, 500-507, 2010.

[17] Xu Rui, Wunsch Donald, Survey of clustering algorithms, IEEE Trans. on Neural Networks, Vol.212, No.3, 645-672, 2005.

[18] Mauricio Maestri, Andrés Farall, A robust clustering method for detection of abnormal situations in a process with multiple steady-state operation modes, Comput. Chem. Eng., Vol.34, No.2, 223-231, 2010.

[19] S. Joe Qin, Donghua Zhou, Gang Li, Total Projection to Latent Structures for Process Monitoring, AIChE J., Vol.56, 168-178, 2010.

[20] S-L.Jamsa Jounela, M. Vermasvuori, A Process Monitoring System Based on the Konohen Self-organizing Maps, Control Engineering Practice, Vol.11, 83-92, 2003.

[21] Shatin, Tuen Mun, Expanding Self-organizing Map for data visualization and cluster analysis, Information Sciences, Vol.163, 157-173, 2004.

[22] B. Lamrini EI-K. Lakhal, M-V. Le Lann, L. Wehenkel, Data validation and missing data reconstruction using self-organizing map for water treatment, Neural Comput & Applic., Vol. 20, No.4, 575-588, 2011.

[23] P. R. Lyman, C. Georgakis, Plant-wide control of the Tennessee Eastman problem, Comput. Chem. Eng., Vol.19, No.3, 321-331, 1995.